
Journal of Computer-Aided Materials Design, **8:** 193–202, 2001.
KLUWER/ESCOM

Ab-initio studies of pressure induced phase transitions in BaO

MUSTAFA ULUDOĞAN*, TAHIR ÇAĞIN, ALEJANDRO STRACHAN and WILLIAM A. GODDARD III
Materials and Process Simulation Center, Beckman Institute (139-74), California Institute of Technology, Pasadena, CA 91125, U.S.A.

Received 22 March 2001; Accepted 8 July 2001

Abstract. We use *ab-initio* Quantum Mechanics to study the zero temperature phase diagram of BaO. We calculate zero temperature Equations of State of different crystalline phases [B1 (NaCl), B8(NiAs), B2(CsCl), and distorted B2] using Density Functional Theory (DFT) with the generalized gradient approximation (GGA). We find the B1 structure to be the thermodynamically stable one at zero pressure; followed by three pressure induced phase transitions. We find that at $P = 11.3$ GPa BaO transforms from B1 to B8; at $P = 21.5$ GPa from B8 to distorted B2. The distorted B2 phase continuously approaches the B2 structure, the phase transformation occurs at $P = 62$ GPa. We also study the band structure of BaO in its high pressure (B2) phase. For $P = 60.5$ GPa, we find a band gap of 3.5 eV in agreement with experimetal value. We find metallization at $P = 230.6$ GPa.

Keywords: Alkaline-earth oxides, Equation of state, Metallization, Phase transformation

1. Introduction

BaO is a well-known alkaline-earth oxide. The high pressure behavior of this oxide is important from the point of view of geophysics; it is an important component of the earth's lower mantle (few kilometers depth) where pressures reach up to 140 GPa. BaO is also a constituent of the ferroelectric material $BaTiO_3$ with great technological importance. Undertanding and modeling the mechanical and electronic properties of BaO (including pressure induced structural phase transformations) is, thus, of great importance.

The alkaline-earth oxides, MgO, CaO, SrO, and BaO, are known to be found in B1 (NaCl) phase at zero stress [1–9]. Most of them undergo a pressure induced phase transition from B1 phase to B2(CsCl). On the other hand, for BaO the low pressure (B1) structure and the high pressure one (B2) are separated by other intermediate crystalline phases. Experiments show a phase transition from the B1 phase transforms to B8 (NiAs) at a pressure of 9.2 GPa [10, 11]. The B8 structure then transforms to distorted B2; experimental pressures for this phase transition are 18 GPa [10] and 14 GPa [11]. Experiments also show that the distorted B2 phase approaches B2 with increasing pressure but the perfect B2 phase was never obtained.

To date, the theoretical studies (to best of knowledge) have covered the phase transformations in BaO as B1 phase to B2 phase. As pointed above, the transition pathway follows the sequence B1-B8-distorted B2-B2. In this work, we present the first study of the full transition path in detail. We have especially analyzed the transition zone by pointwise optimization with *c/a* ratio and the distortion are used as parameters (explained in the next section).

*Permanent address: Department of Physics, Middle East Technical University, 06531, Ankara, Turkey.

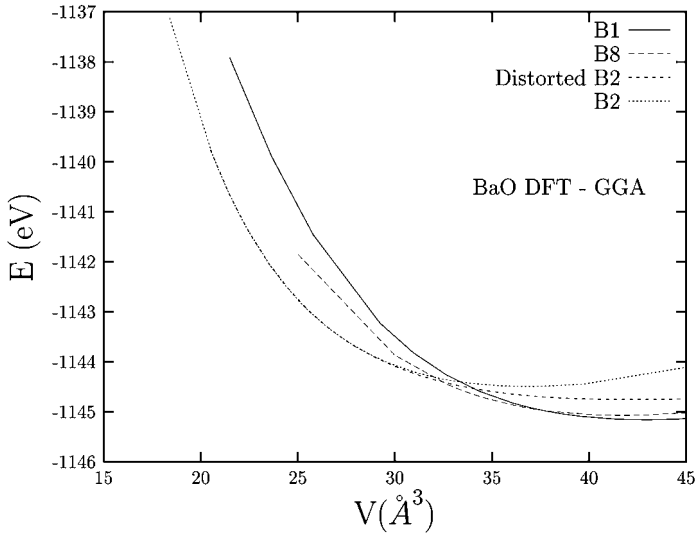

Figure 1. Energy as a function of volume for B1, B8, distorted B2 and B2 phases of BaO from ab initio calculations using DFT-GGA.

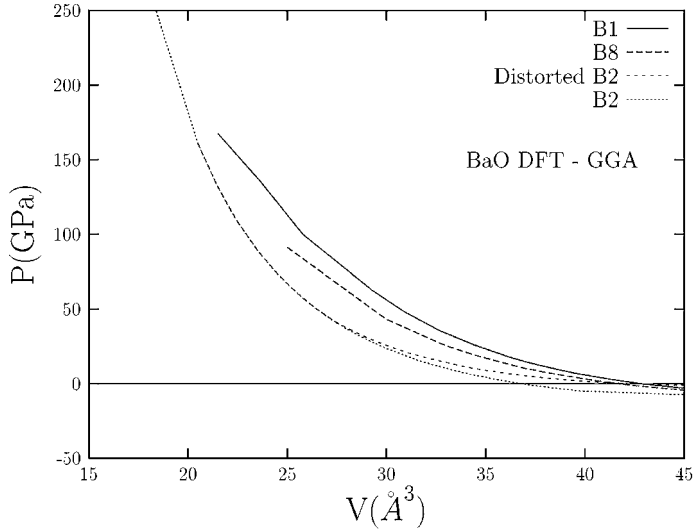

Figure 2. Pressure as a function of volume for B1, B8, distorted B2 and B2 phases of BaO from ab initio calculations using DFT-GGA.

In the following, we present the zero temperature full EOS of BaO which is obtained using the *ab initio* program CASTEP. Furthermore, we have investigated the metallization of BaO under high pressure. Finally, in Section 3, we discuss our results.

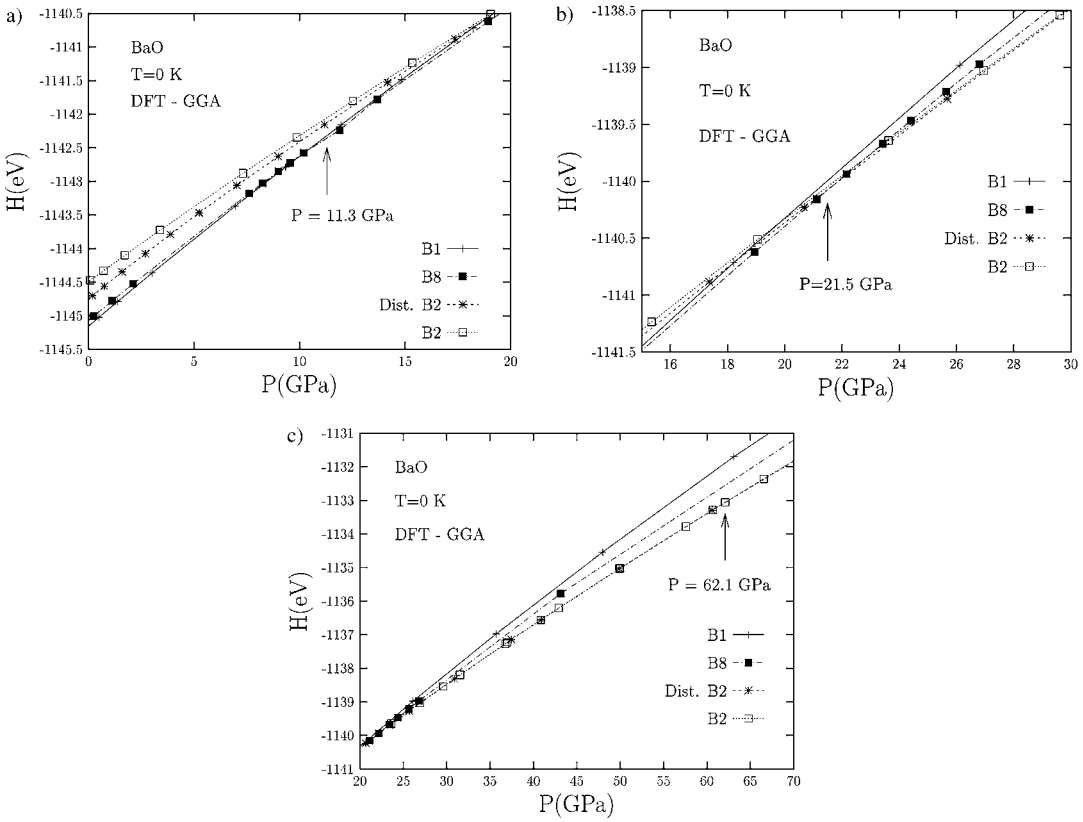

Figure 3. (a) Enthalpy as a function of pressure for the DFT-GGA calculations between the pressure range 0–20 at 0 K. (b) Enthalpy as a function of pressure for the DFT-GGA calculations between the pressure range 15–30 GPa at 0 K. (c) Enthalpy as a function of pressure for the DFT - GGA calculations between the pressure range 20–70 GPa at 0 K.

2. DFT calculations

2.1. Zero temperature equations of state

We present ab-initio Quantum Mechanical calculations of the EOS of different phases of BaO using DFT in the GGA approximation; our calculations correspond to zero temperature except that the zero point energy of the crystal is not considered. We use DFT [12–14], using PW-91 GGA for the exchange and correlation energy functional [15]. *k* points are sampled using $5 \times 5 \times 5$ Monkhorst–Pack mesh. Ultrasoft pseudopotentials are used for both Ba and O [16].

In Figs. 1 and 2, we show the zero temperature EOS of the different crystalline phases of BaO, namely B1(NaCl), B8(NiAs), B2(CsCl) and distorted B2. Fig. 1 shows energy-volume curves and Fig. 2 shows pressure as a function of volume. We have calculated the EOS in a wide volume range, typically between 8% expansion and 50% compression. The distorted B2 phase is tetragonal with two degrees of freedom for constant volume: (i) the *c/a* ratio; and (ii) the distortion in the fractional coordinates of Ba atoms in *z*-direction. O atom is located at (0,0,0) while Ba atom is located at $(0,0.5,0.5+\Delta)$. To study the changes of crystal structure at distorted B2 phase with respect to pressure, we minimized the total energy of BaO crystal with respect to c/a and Δ at each volume keeping the pressure hydostatic.

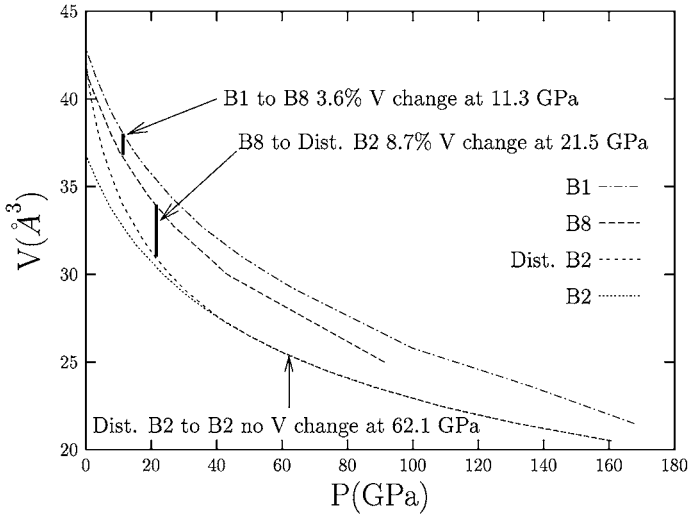

Figure 4. Variation of volume with pressure for B1, B8, distorted B2 and B2 phases of BaO.The percentage change in volume at phase transformation points is also shown.

The EOS parameters were obtained by fitting our DFT-GGA data to Rose's Universal binding curve [17]:

$$E_{\mathrm{EOS}}(a^*) = -E_{\mathrm{coh}}(1 + a^* + ka^{*3})e^{-a^*}, \tag{1}$$

where

$$a^* = \frac{a - a_0}{a_0\lambda}, \tag{2}$$

$$\lambda = \sqrt{\frac{E_{\mathrm{coh}}}{9\Omega_0 B}}, \tag{3}$$

$$k = \frac{\lambda(B' - 1)}{2} - \frac{1}{3}, \tag{4}$$

$$B' = \left(\frac{\mathrm{d}B}{\mathrm{d}P}\right)_{P=0}. \tag{5}$$

Here, the constants a_0, E_{coh}, Ω_0, and B are the lattice parameter, cohesive energy, zero pressure volume, and bulk modulus, respectively. The parameter k depends on the pressure derivative of the bulk modulus evaluated at zero pressure.

EOS parameters, calculated zero pressure volume for B1 ($V_0 = 42.898$ Å) and the experimental value extrapolated to zero temperature ($V_0 = 42.141$ Å) are in good agreement (1.7% difference). All extensive quantities in this paper are given per formula unit (BaO). The calculated cohesive energy (E_{coh}) and isothermal bulk modulus B_T and its derivative with respect to pressure (B'_T) are also in good agreement with experimental results. Table 1 shows EOS parameters obtained in this work for the different phases, together with experimental values and previous theoretical calculations using different models. potential-induced breathing model (Mehl et al. [3]), ionic potentials (Jog et al.[1]), DFT-LDA (Cortona et al. [7]),

Table 1. EOS parameters, bulk modulus, B, and its pressure derivative B′, and elastic constants, $C_S = (C_{11} - C_{12})/2$ and C_{44} for the B1, B8, distorted B2 and B2 phases for BaO. The experimental values are the values extrapolated from room temperature to 0 K. The volumes here are the volumes which correspond to one BaO molecule

Phase	V_0 (Å^3)	E_{coh} (eV)	λ	k	B_0 (GPa)	B_0'	C_S (GPa)	C_{44} (GPa)
B1 experiment	42.141 [18]	10.15 [19]			75.6 [20]	5.67 [21]	45.5 [21]	36.0 [21]
B1 (this work)	42.898	11.01	0.2532	0.1125	71.22	4.52	44.85	39.78
PIB-model [3]	41.367				66.33	4.55		
Ionic pot. I [1]	42.508				73	1.51		
Ionic pot. II [1]	42.970				91	4.17		
DFT-LDA (non-Spherical) [7]	40.026	11.0			73			
DFT-LDA (spherical) [7]	42.049	10.6			68			
LAPW [7]	40.247				86			
LMTO [2]	41.821	12.4			70			
B8 (this work)	41.651	10.45	0.2562	0.0752	68.04	4.19	67.92	30.88
Dist. B2 (this work)	42.211	10.61	0.4060	0.0000	27.13		42.12	74.57
B2 (this work)	36.808	12.44	0.2837	0.1024	74.69	4.07	108.23	3.20

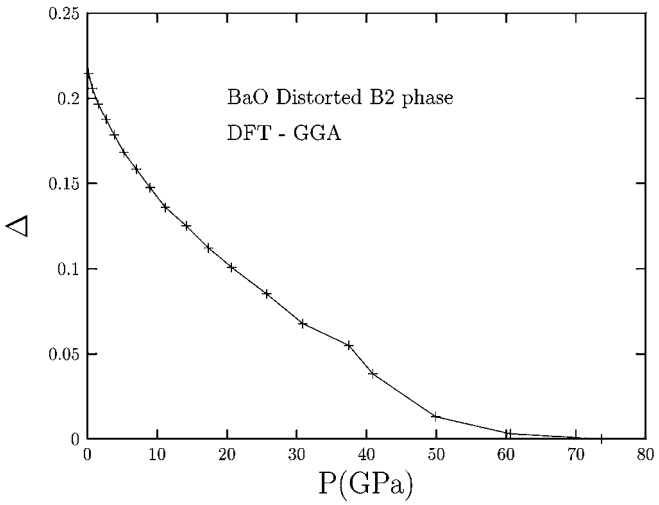

Figure 5. Δ, z-position difference from $z = 0.5$ position with respect to pressure in distorted B2 phase.

linearized-augmented plane-wave (LAPW) (Mehl, a private communication given in Cortona et al. [7]), and linear-muffin-tin orbitals (LMTO) (Springborg et al. [2]).

We have also calculated the elastic constants for B1-BaO by straining the cubic B1 lattice with volume conserving deformations.We obtain $C_s = (C_{11} - C_{12})/2$ using a tetragonal strain:

$$a_T = a_0(1 + \epsilon, 0, 0), \tag{6}$$

$$b_T = a_0(0, 1 + \epsilon, 0), \tag{7}$$

$$c_T = a_0(0, 0, 1/(1 + \epsilon)^2). \tag{8}$$

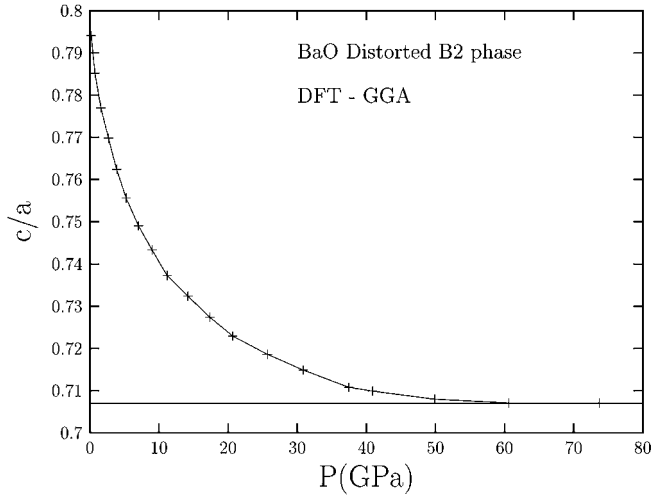

Figure 6. The *c/a* ratio for the distorted B2 phase as a function of pressure. The value of $1/\sqrt{2}$ which corresponds to the B2 structure is shown by a straight line.

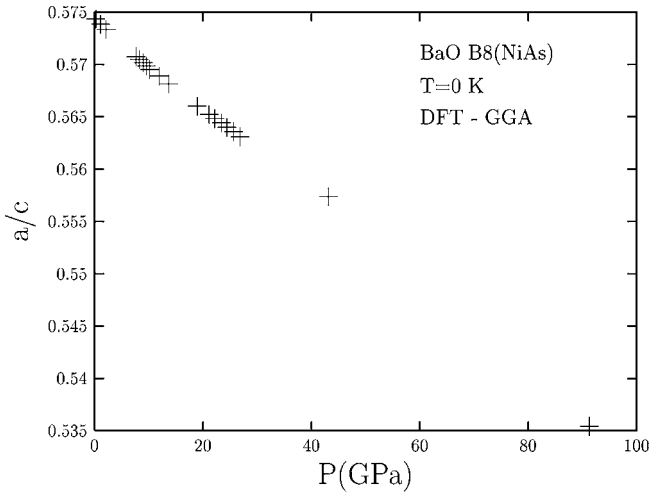

Figure 7. The *c/a* ratio for the B8 (NiAs) phase as a function of pressure.

C_s is obtained from the deformation energy,

$$E = E_0 + 6V_0C_s\epsilon^2. \tag{9}$$

Here, a_0 is the zero stress lattice constant of the system, and a_T, b_T, and c_T are the tetragonal strained cell vectors; ϵ is the applied strain, E_0 is the energy of the unstrained system and V_0 is the zero stress volume.

For C_{44}, we use an orthorombic strain:

$$a_O = a_0(\sqrt{1+\epsilon^2}, 0, 0), \tag{10}$$

$$b_O = a_0(0, \sqrt{1+\epsilon^2}, 0), \tag{11}$$

$$c_O = a_0(0, 0, 1/(1-\epsilon^2)). \tag{12}$$

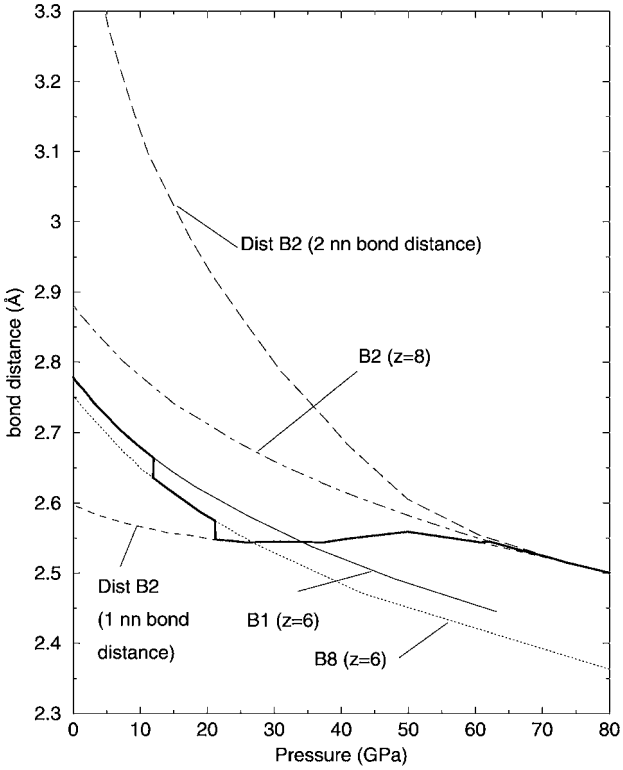

Figure 8. Bond distance between Ba and O atoms as a function of pressure at experimentally stable phases B1, B8, distorted B2 and B2 of BaO.

a_O, b_O and c_O are the orthorombic strained lattice vectors. C_{44} is obtained from the following deformation energy relation:

$$E = E_0 + 2V_0 C_{44}\epsilon^2. \tag{13}$$

Table 1 also shows the calculated elastic constants which are in very good agreement with experimental values.

2.2. Pressure induced phase transitions in BaO

Two experiments performed at ambient temperature [10, 11] show that phase transitions occur from B1 phase to B8 phase at the a pressure $P = 9.2$ GPa and from B8 phase to distorted B2 phase at the pressures 18 GPa and 14 GPa, respectively. The phase transition from distorted B2 structure to B2 structure has not been observed experimentally up to pressure $P = 60.5$ GPa.

Figs. 3a–c show the calculated enthalpy $H = U + PV$, for the different phases in different pressure ranges which allow the identification of the phase transformations. Our DFT-GGA calculations show the B1-B8 transitions at $P = 11.3$ GPa (Fig. 3a). B8 transforms to distorted B2 at $P = 21.5$ GPa. (Fig. 3b). Finally we find that distorted B2 continuously transforms to B2 at $P = 62.1$ GPa (Fig. 3c). Table 2 summarizes the our results regarding the transition pressures together with experimental values. Our DFT-GGA data predicts the correct order of phases as the pressure is increased and overestimates the transition pressures. The differences of the transition pressures between the experiments and theory may be due to: (i) our calculations correspond to $T = 0$ K whereas the experiments were done at room temperature; (ii)

Table 2. Experimental and theoretical phase transitions from B1 phase to B8 phase, from B8 phase to distorted B2 phase and from distorted B2 phase to B2 phase. Theoretical results are 0 K results, and the experimental results are room temperature results.

Phase transition	B1 to B8 (GPa)	B8 to Dist. B2 (GPa)	Dist. B2 to B2 (GPa)
Experiment I [10]	9.2	18.0	
Experiment II [11]	9.2	14.0	
Theory (this work)	11.3	21.5	62.1

our system is free of any structural defects, and (iii) approximations that are coming from the calculation method such as: GGA method (PW-91) and the pseudopotentials used to replace the core electrons.

In Fig. 4 we show the volume change during the pressure induced phase transitions. At 11.3 GPa, there is a volume decrease of 3.6% when the structure changes from B1 to B8. The volume change is larger for the B8 to distorted B2 phase tranformation at $P = 21.5$ GPa (8.7% volume reduction). The transformation from distorted B2 to B2 involves no volume change at 62.1 GPa. Distorted B2 structure continuously transforms into B2 phase with the increase in the applied pressure. The distorted B2 structure has two internal parameters, (see previous section): Δ and *c/a*. The B2 phase is obtained from the distorted structure with $\Delta = 0$ and $c/a = 1/\sqrt{2}$. Pressure dependence of Δ and *c/a* ratio are plotted in Figs. 5 and 6, respectively. We can see that the B2 structure continuously approaches B2, the phase transition occuring at P=62.1 GPa. As already mentioned this phase transition has not been observed experimentally up to 60.5 GPa. Weir et al. [11] suggested that BaO may adopt the undistorted B2 phase only above 100 GPa in the absence of any intervening first-order transition by assuming a linear extrapolation of his experimental *c/a* plot. B8 structure has only one internal parameter, *a/c* and its pressure dependence which is almost linear as shown in Fig. 7 for completeness.

The last issue for understanding of how phase transitions occur is the bond lengths between Ba and O and the coordination number of these phases as a function of pressure. The results are shown in Fig. 8. The bold line shows the change of the bond distances at stable phases with respect to applied pressure. At zero stress, the coordination number in B1 is 6. At B1 to B8 phase transition point, 11.3 GPa, there is a discontinous decrease in the bond distance of Ba and O atoms. Thus, B8 coordination number still is 6. In distorted B2 phase, the coordination number changes as a function of pressure. Initially it has 4 first nearest neighbors at 2.6 Å and 4 second nearest neighbors at 2.78 Å. These two nearest neighbor shell bond distances reach to same value at 2.56 Å. B2 to B2 phase transition point. Consequently, in B2 phase, coordination number becomes 8.

2.3. METALLIZATION

Pressure induced metallization is another important process in order to characterize the high pressure behavior of BaO. We obtained the bandgap of BaO in the high pressure phase (B2). The results are shown in Fig. 9. At high pressure, it is seen that BaO is metallized since there is no bandgap.

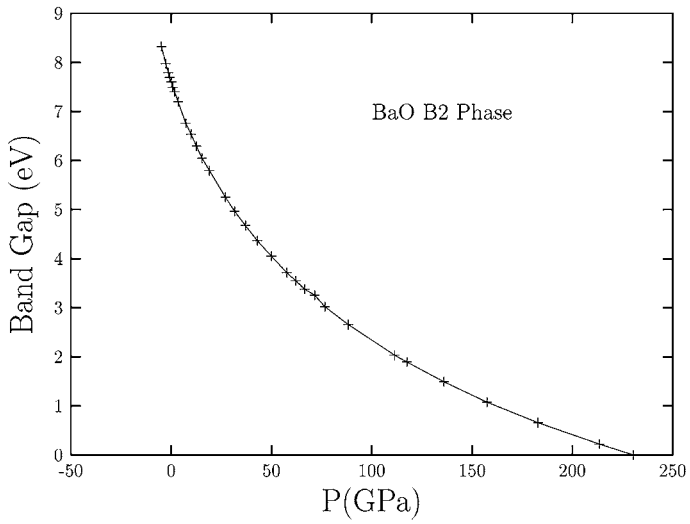

Figure 9. Bandgap of BaO at B2 phase as a function of pressure.

Bukowinski et al. [22] examined theoretically metallization in BaO using augmented plane wave band-structure calculation and he estimated the metallization pressure to be 100 GPa. But Weir et al. [11] suggested that the metallization might occur well above 100 GPa because BaO is transparent and colorless at 60.5 GPa. So, the experimentally determined bandgap [11] is above 3 eV; our *ab-initio* results of 3.5 eV is in agreement with this value at the same pressure. Our results show a continuous decrease of the bandgap with the applied pressure and we obtain metallization at $P = 230.6$ GPa. We claim that there is no discontinuity in the pressure induced bandgap of B2 phase of BaO. Besides our metallization pressure is consistent with the value Weir expected to find (well above 100 GPa).

3. Conclusions

We have calculated the zero pressure EOS of BaO using DFT in the GGA approximation. At zero pressure the thermodynamically stable phase is B1. We identify three pressure induced phase transformations: (i) B1 to B8 at $P = 11.3$ GPa with a volume decrease (at constant pressure) of $\Delta V = 3.6\%$; (ii) B8 to distorted B2 at $P = 21.5$ GPa with $\Delta V = 8.7\%$; the distorted B2 phase continuously approaches B2 with a phase transition at $P = 62.1$ GPa. The First Principles phase diagram is in good agreement with experimental results. The calculated zero temperature B1 to B8 and B8 to distorted B2 transition pressures are $\sim$ 2 GPa higher than the room temperature experimental values. The distorted B2 to B2 phase transition has never been observed experimentally but extrapolation of the meassured *c/a* as a function of pressure leads to an estimation of the phase transition pressure of over 100 GPa [11]; we obtain a pressure of 62.1 GPa for this phase transition.

EOS data for different phases in a wide volume range is invaluable information to derive accurate Force Fields to be used in large scale Molecular Dynamics simulations [9].

We have also calculated the band strucutre of BaO in the high pressure B2 phase. We calculate pressure induced metallization at $P = 230.6$ GPa; in agreement with the value that experimentalists suggested to obtain.

Acknowledgements

This research was funded in part by the DOE-ASCI-ASAP, NSF-CSEM and ARO-MURI programs. M.U. would like to thank Scientific and Technical Research Council of Turkey for supporting his stay at the MSC. The facilities of the Materials and Process Simulations Center used in these studies were funded by the NSF-MRI, DURIP, and the Beckman Institute. In addition, the Materials and Process Simulations Center is funded by grants from the ARO-MURI, NSF, NIH, Avery-Dennison, Asahi Chemical, Chevron, 3M, Dow Chemical, General Motors, Nippon Steel, Seiko-Epson, and Kellogg's.

References

1. Jog, K.N., Singh, R.K. and Sanyal, S.P., Phys. Rev. B31 (1985) 6047.
2. Springborg, M. and Taurian, O., J. Phys. C.: Solid State Phys. 19 (1986) 6347.
3. Mehl, M.H., Hemley, R.J., Boyer, L.L., Phys. Rev. B33 (1986) 8685.
4. Jog, K.N., Sanyal, S.P. and Singh, R.K., Phys. Rev. B35 (1987) 5235.
5. Mehl, M.J., Cohen, R.E. and Krakuer, H., J. Geophys. Res. 93 (1988) 8009.; J. Geophys. Res. 94 (1989) 1977.
6. Kalpana, G., Palanivel, B. and Rajagopalan, R., Phys. Rev. B52 (1995) 4.
7. Cortona, P. and Monteleone, A.V., J. Phys. Condens. Matter. 8 (1996) 8983.
8. Habas, M.-P., Dovesi, R. and Lichanot, A., J. Phys. Condens. Matter. 10 (1998) 6997.
9. Strachan, A., Çağın, T. and Goddard III, W.A., Phys. Rev. B60 (1999) 15084.
10. Liu, L.-G. and Bassett, W.A., J. Geophys. Res. 77 (1972) 4934.
11. Weir, S.T., Vohra, Y.K. and Ruoff, A.L., Phys. Rev. B33 (1986) 4221.
12. Hohenberg, P. and Kohn, W., Phys. Rev. 136 (1964) 864B.
13. Kohn, W. and Sham, L.J., Phys. Rev. 140 (1965) 1133A.
14. Payne, M.C., Teter, M.P., Allan, D.C., Arias, T.A. and Joannopoulos, J.D., Rev. Mod. Phys. 64 (1992) 1045.
15. Perdew, J.P. and Wang, U., Phys. Rev. B46 (1992) 6671.
16. Vanderbilt, D., Phys. Rev. B41 (1990) 7892.
17. Rose, J.H., Smith, J.R., Guinea, F. and Ferrante, J., Phys. Rev. B29 (1984) 2963.
18. Zollweg, R.J., Phys. Rev. 100 (1955) 655.
19. The NBS tables of chemical thermodynamic properties, Selected values for inorganic and C_1 and C_2 organic substances in SI units, Volume 11, 1982, Supplement No. 2 (Published by the American Chemical Society and the American Institute of Physics for the NAtional Bureau of Standards)
20. Kwang-Oh, P. and Sivertsen, J.M., J. Am. Ceram. Soc. 60 (1977) 537.
21. Chang, Z.P. and Graham, E.K., J. Phys. Chem. Solids 38 (1977) 1355.
22. Bukowinski, M.S.T. and Hauser, J., Geophys. Res. Lett. 7 (1980) 689.
23. Rappé, A. and Goddard III, W.A., J. Phys. Chem. 95 (1991) 3358.